European Neuropsychopharmacology 50 (2021) 64–74

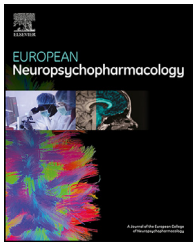

www.elsevier.com/locate/euroneuro

White matter microstructure alterations in cortico-striatal networks are associated with parkinsonism in schizophrenia spectrum disorders

Jakob Wasserthal[a,b], Klaus H. Maier-Hein[a,c], Peter F. Neher[a,b], Robert C. Wolf[d], Georg Northoff[e], John L. Waddington[f], Katharina M. Kubera[d], Stefan Fritze[g], Anais Harneit[h], Lena S. Geiger[h], Heike Tost[h], Dusan Hirjak[g,*]

[a] *Division of Medical Imaging Computing (MIC), German Cancer Research Center (DKFZ), Heidelberg, Germany*
[b] *Medical Faculty Heidelberg, Heidelberg University, Heidelberg, Germany*
[c] *Section of Automated Image Analysis, Heidelberg University Hospital, Heidelberg, Germany*
[d] *Center for Psychosocial Medicine, Department of General Psychiatry, University of Heidelberg,Germany*
[e] *Mind, Brain Imaging and Neuroethics Research Unit, The Royal's Institute of Mental Health Research, University of Ottawa, Ottawa, ON, Canada*
[f] *School of Pharmacy and Biomolecular Sciences, Royal College of Surgeons in Ireland, Dublin, Ireland*
[g] *Department of Psychiatry and Psychotherapy, Central Institute of Mental Health, Medical Faculty Mannheim, Heidelberg University, Mannheim, Germany*
[h] *Department of Psychiatry and Psychotherapy, Research Group System Neuroscience in Psychiatry, Central Institute of Mental Health, Medical Faculty Mannheim, Heidelberg University, Mannheim, Germany*

Received 17 September 2020; received in revised form 15 March 2021; accepted 10 April 2021

KEYWORDS
White matter;
DTI;
Parkinsonism;

Abstract
The specific role of white matter (WM) microstructure in parkinsonism among patients with schizophrenia spectrum disorders (SSD) is largely unknown. To determine whether topographical alterations of WM microstructure contribute to parkinsonism in SSD patients, we examined healthy controls (HC, n=16) and SSD patients with and without parkinsonism, as defined by

* Corresponding author.
E-mail address: dusan.hirjak@zi-mannheim.de (D. Hirjak).

https://doi.org/10.1016/j.euroneuro.2021.04.007

Schizophrenia spectrum disorders; Sensorimotor domain

Simpson-Angus Scale total score of ≥4 (SSD-P, *n*=33) or <4 (SSD-nonP, *n*=62). We used whole brain tract-based spatial statistics (TBSS), tractometry (along tract statistics using TractSeg) and graph analytics (clustering coefficient (CCO), local betweenness centrality (BC)) to provide a framework of specific WM microstructural changes underlying parkinsonism in SSD. Using these methods, post hoc analyses showed (a) decreased fractional anisotrophy (FA), as measured via tractometry, in the corpus callosum, corticospinal tract and striato-fronto-orbital tract, and (b) increased CCO, as derived by graph analytics, in the left orbitofrontal cortex (OFC) and left superior frontal gyrus (SFG), in SSD-P patients when compared to SSD-nonP patients. Increased CCO in the left OFC and SFG was associated with SAS scores. These findings indicate the prominence of OFC alterations and aberrant connectivity with fronto-parietal regions and striatum in the pathogenesis of parkinsonism in SSD. This study further supports the notion of altered "bottom-up modulation" between basal ganglia and fronto-parietal regions in the pathobiology of parkinsonism, which may reflect an interaction between movement disorder intrinsic to SSD and antipsychotic drug-induced sensorimotor dysfunction.

1. Introduction

Despite considerable phenomenological and neuroimaging research on sensorimotor and psychomotor abnormalities intrinsic to schizophrenia spectrum disorders (SSD) (Hirjak et al., 2018a, 2018b, 2018c, 2015a; Walther et al., 2020), in association with movement disorder induced by antipsychotic drugs, little attention has been paid to parkinsonism (Molina et al., 2018; Pappa and Dazzan, 2009). From a clinical perspective, parkinsonism is a psychomotor syndrome characterized by rigidity, tremor, bradykinesia and occasionally positive glabellar tap sign or increased salivation (Cuesta et al., 2014; Peralta et al., 2012), and is present in SSD among antipsychotic-naïve (median prevalence 17%) as well as antipsychotic-treated (prevalence 15-30%) patients (Cuesta et al., 2014; Peralta et al., 2012; Waddington, 2020; Whitty et al., 2009). This challenge has been brought into sharp focus by recent evidence that SSD and Parkinson's disease share genetic architecture, with overlapping risk loci (Smeland et al., 2021), which indicates some overlap in neuronal network pathobiology. The majority of magnetic resonance imaging (MRI) studies have repeatedly pointed to prominent striatal contributions (Northoff, 2002) and disturbed structure/function-coupling in cortical and subcortical systems subserving coordinated sensorimotor behavior (Wolf et al., 2020a), suggesting an aberrant "bottom-up modulation" (Northoff, 2002) of cortical-subcortical sensorimotor circuits (Wolf et al., 2021; Fritze et al., 2021). However, the relative contribution of regional white matter (WM) changes (e.g. degeneration of WM tracts) to parkinsonism in SSD remains to be clarified.

Here, we combined three distinct diffusion-tensor imaging (DTI) analysis techniques based on diffusion MRI (dMRI) to examine WM microstructural alterations underlying parkinsonism in SSD. First, we used Tract-Based Spatial Statistics (TBSS) (Smith et al., 2006). Since TBSS has difficulties in accurately aligning fiber tracts due to variation in tract size and shape (Wassermann et al., 2011; Yeatman et al., 2011), in a second step we used a recently developed comprehensive approach (TractSeg) (Wasserthal et al., 2019). This allows accurate reconstruction of fiber tracts in subject space, thus avoiding the problem of inaccurate co-registration for tracts of varying size and shape. In particular, we evaluated fractional anisotropy (FA) along each of the 15 neurobiologically plausible tracts (often referred to as Tractometry) that represent important connections between sensorimotor regions [corpus callosum (rostrum (CC_1), genu (CC_2), rostral body (CC_3), anterior midbody (CC_4), posterior midbody (CC_5), isthmus (CC_6), splenium (CC_7), as well as bilateral corticospinal (CST), thalamo-premotor (T_PREM), striato-fronto-orbital (ST_FO), and striato-premotor (ST_PREM) tracts]. Finally, we focused on variations in the structural connectome underlying parkinsonism in SSD by employing the concepts of local network clustering coefficient (CCO, i.e. the ratio of total number of edges among the neighbors of the node (region) to the total number of edges that can exist among the neighbors of the node per node (Goch et al., 2014), and local network betweenness centrality (BC, i.e. the number of shortest paths from all vertices to all others that pass through that node (Freeman, 1977) in psychomotor regions [orbitofrontal cortex (OFC), primary motor area (M1), supplementary motor area (SMA), superior parietal cortex (SPC), thalamus, caudate and putamen] identified by previous studies on parkinsonism in SSD (Waddington, 2020; Wolf et al., 2020b).

2. Methods

2.1. Patients

Initially, we examined a total of 111 right-handed (Oldfield, 1971) patients satisfying DSM-IV-TR (Sass et al., 2003) criteria for schizophrenia (n = 104) or schizoaffective disorder (n = 7) (Hirjak et al., 2019, 2020) and 28 healthy control subjects (HC). Inclusion and exclusion criteria are listed in Supplementary Information. This study was approved by the Research Ethics Committee of the Medical Faculty at Heidelberg University, Germany. Written informed consent was obtained from all SSD patients and HC after the aims and procedures of the study had been fully explained.

2.2. Clinical assessment

SSD patients were recruited and examined within one week after partial remission of psychotic symptoms. The duration between

evaluation of psychopathology, motor assessment and MRI examination was less than 3 days. At the time of examination none of the SSD patients were taking benzodiazepines or anticholinergic medication and all patients were on stable antipsychotic medication for at least two weeks (for details on antipsychotic medication see Supplementary Information). Daily doses of antipsychotic medication were converted to olanzapine equivalents (OLZ) according to the classical mean dose method (Leucht et al., 2015). For assessment of parkinsonism we used the Simpson-Angus Scale (SAS) (Simpson and Angus, 1970); for details on SAS domains see Supplementary Information).

We then excluded 16 SSD patients from the original study sample (111−16=95) to create two well-balanced (in terms of age, sex, education and OLZ-equivalent dose) groups of SSD patients with parkinsonism (SSD-P; SAS total score ≥ 4, n=33) and without parkinsonism (SSD-nonP; SAS<4, n=62) according to Cuesta et al. (2014). The patient groups were carefully matched with respect to sex and education, because both variables can influence sensorimotor functioning in SSD (Molina et al., 2018; Peralta et al., 2012). Similarly, we excluded 12 HC from the original sample (28−12=16) to create a well-matched (in terms of age, sex and education) control group (n=16). Additionally, we followed a correlative approach, assuming dimensional symptom expression along a neurobiological continuum in SSD patients with various degrees of parkinsonism (n=95) (Dazzan et al., 2004).

2.3. MRI data acquisition

MRI scans were acquired at the Central Institute of Mental Health, University of Heidelberg, on a 3.0 T Magnetom TIM Trio MR scanner (Siemens) equipped with a 32 channel multi-array head-coil. Technical details on MRI sequences are provided as Supplementary Information.

2.4. Image processing

2.4.1. Preprocessing

The brain was extracted from T1 images and bias field was corrected using FMRIB Software Library (FSL) (Jenkinson et al., 2012; Woolrich et al., 2009). Diffusion-weighted images (DWI) were denoised (MRtrix dwidenoise) (Veraart et al., 2016), corrected for Gibbs ringing artifacts (MRtrix mrdegibbs) (Kellner et al., 2016), corrected for eddy currents and head motion (FSL eddy) (Andersson and Sotiropoulos, 2016), corrected for bias field (MRtrix dwibiascorrect) (Tustison et al., 2010) and brain masked (FSL bet) (Smith, 2002). Using FSL FLIRT (Jenkinson and Smith, 2001) the DWI images were rigidly registered to Montreal Neurological Institute space. Then the T1 images were rigidly aligned with the DWI images. Finally, all images were manually inspected and only those images for which this pre-processing pipeline was successful were retained.

2.4.2. Data and statistical analyses (for overview see Fig. 1)

TBSS: In order to detect global patterns of WM variations, we followed the recent recommendation regarding TBSS (Bach et al., 2014) and registered all subjects to a common space using tensor-based registration with DTI-TK (http://www.nitrc.org/projects/dtitk). Details on the TBSS (Smith et al., 2006) processing steps are provided in Supplementary Information. Additionally, for each of the bundles between sensorimotor regions (CC_1-7, CST, T_PREM, ST_FO, and ST_PREM) that were also used for the Tractometry analysis we averaged the FA values of the TBSS WM skeleton within the bundle mask (as generated with TractSeg). These aggregated FA values were used for additional between-group analyses to be comparable with Kelly and colleagues (Kelly et al., 2018). The statistical analysis of the aggregated FA is identical to analysis of the large-scale network analysis.

Tractometry: Along-tract statistics of FA (Tractometry) were computed using TractSeg (Wasserthal et al., 2018, 2019). TractSeg generates bundle-specific tractograms and then analyzes FA along 100 points of each bundle (further details are provided in Supplementary Information). Statistics such as T-tests and correlations can be calculated point-wise along these 100 points. The permutation-based multiple comparison correction (with n=5000 repetitions) published by Nichols and Holmes (Nichols and Holmes, 2002; Yeatman et al., 2012) was used to appropriately correct p values for the 100 tests, given the correlation structure of the data. An uncorrected significance threshold of $p < 0.05$ was used, with the corrected p-value being different for each bundle depending on its correlation structure. Covariates were controlled by regressing them out of the data before performing each t-test (categorical approach) or correlation (dimensional approach).

Large-scale network analysis: We performed whole brain tractography according to recommendations given following evaluation of fiber tracking algorithms (Neher et al., 2015); details are provided in Supplementary Information. While tractography-based methods typically analyse specific structures of interest, graph-based large-scale network analysis of the connectome can provide detailed measures of larger-scale architectural patterns in the brain (Goch et al., 2014; Rubinov and Bullmore, 2013). To construct a graph representation, we used the T1 image to create a parcellation of the brain using FreeSurfer (http://surfer.nmr.mgh.harvard.edu/) (Dale et al., 1999; Fischl and Dale, 2000; Fischl et al., 1999) and the atlas of Destrieux (Desikan et al., 2006; Fischl et al., 2004; Segonne et al., 2004); details on the FreeSurfer processing steps are provided in Supplementary Information. Consecutively, we constructed connectomics networks based on the tractography result and then brain parcellation using MRtrix (Smith et al., 2015). The normalized CC and BC for 7 nodes (OFC, M1, SMA, SFG, thalamus, caudate, and putamen) located in both hemispheres were computed. In the next step, homogeneity of variance in CC and BC values was clarified using Levene's Test. Then, we conducted one-way ANOVAs followed by post-hoc analyses using Tukey's test to assess differences in aggregated FA, CC and BC values of sensorimotor regions between SSD-P, SSD-nonP and HC. We also included additional between-group ANCOVAs, controlling for (i) age, sex, OLZ and PANSS-N and (ii) age, sex and OLZ, that compared SSD-P and SSD-nonP with 16 right-handed HC matched for age and sex. For the dimensional approach across all SSD patients (n=95; two-tailed partial correlation) we controlled for age, sex, OLZ and PANSS-N, because these variables have been used in previous studies and might have an impact on SAS scores and DTI measures.

Finally, p values for identified between-group differences and associations were corrected for multiple comparison using the Bonferroni method. The corrected threshold for aggregated FA was set to $p = 0.002$ [$\alpha = 0.05/30$ tests (15 tracts $\times$ 2 approaches (dimensional and correlational)]. The corrected threshold for tractometry was set depending on the family-wise error (FWE)-corrected significance threshold within the respective WM tract [α = alphaFWE value/30 tests (15 tracts $\times$ 2 approaches (dimensional and correlational)]. The corrected threshold for large-scale network analysis was set to $p = 0.0009$ [$\alpha = 0.05/56$ tests (7 regions of interest $\times$ 2 hemispheres $\times$ 2 approaches (dimensional and correlational) $\times$ 2 metrics (CC and BC))].

3. Results

3.1. Clinical and demographical data

Demographic and clinical data are shown in Table 1. While SSD-P patients were receiving slightly higher current daily

Table 1 Demographics and clinical scores for schizophrenia spectrum disorders patients (n=95) divided into SSD-nonP (SAS total score <4; n=62) and SSD-P (SAS total score ≥4, n=33) groups and healthy controls (HC, n=16).

Variable/study group	SSD-nonP (n=62)	SSD-P (n=33)	HC (n=16)	t[1]/F[3]	df	Sig.
Age	41.1 ± 9.6	39.8 ± 11.1	40.2 ± 14.4	0.612/ 0.176	93/ 110	0.542/0.839
Sex (m/f)[2]	31/31	20/13	10/6	0.458/0.974	1/2	0.499/0.324
Education (years)	13.3 ± 2.7	13.3 ± 3.0	13.6 ± 2.0	−0.125/0.082	93/110	0.901/ 0.922
Olanzapine equivalents	17.3 ± 9.00	19.5 ± 11.3	0	−1.007/37.708[4]	93/2[4]	0.316/<0.001[4]
DOI (years)	11.0 ± 10.4	12.5 ± 12.1	–	−0.634	93	0.528
GAF score	71.8 ± 16.3	67.6 ± 16.4	–	1.19	93	0.237
PANSS						
Positive	16.1 ± 7.5	13.4 ± 5.7	–	1.828	93	0.071
Negative	15.1 ± 6.9	17.7 ± 7.9	–	−1.644	93	0.103
Global	35.1 ± 11.6	33.0 ± 8.8	–	0.931	93	0.354
Total	66.3 ± 21.8	63.8 ± 17.3	–	0.562	93	0.575
BPRS total score	37.8 ± 13.7	33.6 ± 9.1	–	1.558	93	0.123
SAS						
Hypokinesia	0.35 ± 0.48	1.06 ± 0.7	–	−5.76	93	<0.001
Rigidity	0.26 ± 0.51	2.52 ± 2.12	–	−7.983	93	<0.001
Tremor	0.37 ± 0.48	0.94 ± 0.74	–	−4.473	93	<0.001
Glabella- Salivation	0.55 ± 0.67	1.27 ± 0.91	–	−4.415	93	<0.001
Total score	1.50 ± 1.11	5.76 ± 2.15	–	−12.744	93	<0.001
AIMS total	0.91 ± 2.03	1.27 ± 3.09	–	−0.634	93	0.527
TMT-B	118.2 ± 65.0	103.2 ± 63.5	–	1.083	93	0.282

[1] The *t* values were obtained using two-tailed independent samples *t*-test between patient groups.
[2] The *p*-values for distribution by sex were obtained by chi-square test between the two patient and across the three study groups.
[3] The *F*-values and *p*-values were obtained using ANOVA between the two patient and across the three study groups.
[4] The H-values and *p*-value were obtained using a Kruskal-Wallis non-parametric test across the three study groups.
Statistically significant ($p<0.05$) results are in bold.
Abbreviations: SD: standard deviation; df: degree of freedom; DOI: Duration of illness; GAF: Global assessment of functioning (GAF-Skala: Global Assessment of Functioning Scale in: Diagnostische Kriterien und Differentialdiagnosen des diagnostischen und statistischen Manuals psychischer Störungen DSM-III.R.-Weinheim; Basel: Beltz, 1989); PANSS: The Positive and Negative Syndrome Scale; BPRS: Brief Psychiatric Rating Scale; SAS: Simpson-Angus Scale; AIMS: Abnormal involuntary movement scale; TMT-B: Trail Making Test B.

doses of antipsychotics and showed slightly greater severity of negative symptoms than SSD-nonP patients, these numerical differences failed to attain statistical significance. There was no significant association ($p<0.05$, two-tailed) between OLZ and SAS score either in the SSD-P (all *p*-values>0.22) or in the SSD-nonP group (all *p*-values>0.08). In a pooled analysis (SSD-P + SSD-nonP; $n=95$), there was no significant association ($p<0.05$, two-tailed) between OLZ and SAS score (all *p*-values>0.25). Nevertheless, we proceeded conservatively and included age, sex, OLZ and PANSS-N as covariates in the analyses.

3.2. Categorical analyses

TBSS: First, standard TBSS analyses indicated a nominal reduction of FA in SSD-P patients compared to SSD-nonP patients, but this difference did not attain statistical significance ($p=0.12$). Second, we performed an aggregated TBSS using the average FA across the 15 tracts between sensorimotor regions. Homogeneity of variances was confirmed using Levene's Test, which showed indistinguishable variance in FA values across sensorimotor regions (*p*-values > 0.05) other than CC_1 ($p=0.006$) and the left ST_FO ($p=0.003$). The FA values in CC_7 ($F_{(2,\ 108)}=3.32$, $p=0.04$) and left ST_FO ($F_{(2,\ 108)}=3.29$, $p=0.04$) showed a significant main effect of group. Third, post-hoc Tukey's tests revealed significant differences in FA for CC_7 ($p=0.03$) and right ST_FO ($p = 0.04$) within the three groups (SSD-P < SSD-nonP < HC). Fourth, ANCOVA revealed significantly reduced FA in the left ST_FO ($F_{(1,\ 89)}=4.04$, p=0.04) in SSD-P patients compared to SSD-nonP patients. Thus, these p-values did not survive Bonferroni correction for multiple testing (threshold at $p=0.002$).

Tractometry: In terms of along-tract statistics (Tractometry) using TractSeg, we found significantly decreased FA in CC_7 (min. *p*-value<0.002), left CST (min. *p*-value<0.0007) and ST_FO (min. *p*-value<0.003) in SSD-P patients compared to SSDnonP patients. Thus, the minimal *p*-values did not survive Bonferroni correction for multiple testing (threshold for CC_7 at $p=0.001/30=0.00003$; for left CST at $p=0.001/30=0.00003$ and left ST_FO at $p=0.004/30=0.0001$).

Large-scale network analysis: Levene's Test showed indistinguishable variances in CCO and BC values across all sensorimotor regions (all *p*-values > 0.05). The CCO values in the left OFC ($F_{(2,\ 108)} = 3.38$, $p = 0.03$) showed a significant main effect of group and CCO values in the left SFG ($F_{(2,\ 108)}=2.986$, $p=0.05$) showed a marginally significant main effect of group (Supplementary Table 1). Tukey post-hoc analysis revealed significantly higher CCO values in the left SFG ($p=0.043$) and marginally higher CCO values in the left OFC ($p=0.05$) in SSD-P patients compared to SSD-nonP patients. Furthermore, ANCOVA revealed signifi-

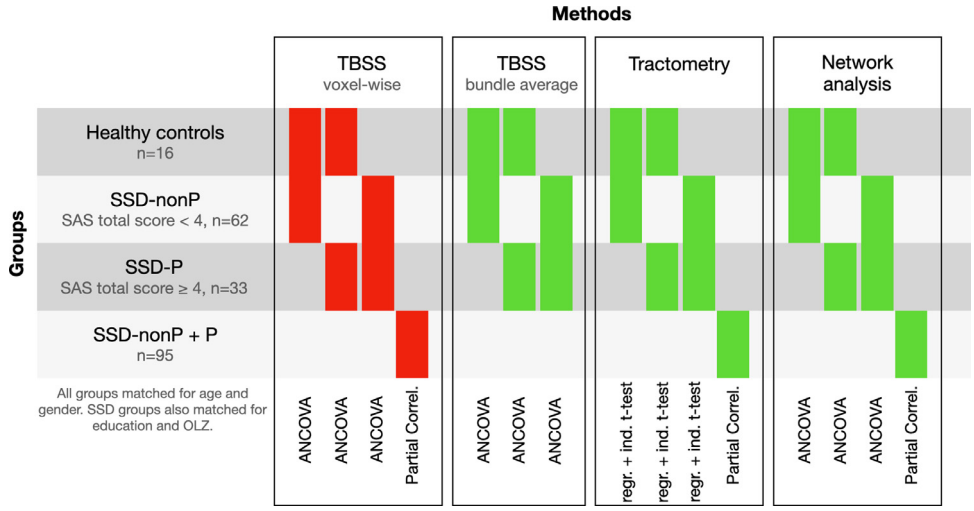

Fig. 1 Overview of the different analyses in this study. Colored bars indicate which groups are compared by the respective test. The color shows if the test gave significant results ($p<0.05$) (green) or not (red) (results before Bonferroni correction). (Abbreviations: SSD: schizophrenia spectrum disorders, reg. + ind. *t*-test: regressing out covariates + independent *t*-test, Partial Correl.: partial correlation.) (For interpretation of the references to color in this figure legend, the reader is referred to the web version of this article.)

cantly higher CCO values in SSD-P sample compared to SSD-nonP patients in the left OFC ($F_{(1,\ 89)}=8.95$, $p=0.004$) and left SFG ($F_{(1,\ 89)}=4.77$, $p=0.03$). Thus, these *p*-values did not survive Bonferroni correction for multiple testing (threshold at $p=0.0009$).

3.3. Dimensional analyses

TBSS: We found no significant association between SAS scores and FA (voxel-wise TBSS; all *p*-values>0.05). Using partial correlation, we found no significant association between SAS score and average FA for CC_7 or left and right ST_FO in the entire patient sample ($p>0.1$). After excluding all four covariates (age, sex, OLZ and PANSS-N), there was still no significant association between SAS scores and FA in the entire patient sample ($p>0.08$).

Tractometry: We found significant negative associations between SAS total scores and FA in CC_5 (min. *p*-value<0.0004), left (min. *p*-value<0.00006) and right (min. *p*-value<0.0004) CST and left (min. *p*-value<0.002) and right (min. *p*-value<0.002) ST_FO (Fig. 2; all *p*-values were below the alphaFWE-corrected threshold). Thus, the minimal *p*-values did not survive Bonferroni correction for multiple testing (threshold for CC_5 at $p=0.001/30=0.00003$; for left CST at $p=0.001/30=0.00003$, for right CST at $p=0.001/30=0.00003$, for left ST_FO $p=0.003/30=0.0001$ and for right ST_FO $p=0.004/30=0.0001$).

Large-scale network analysis: We identified a significant relationship (two-tailed partial correlation) between SAS total score and CCO in the left OFC ($r=0.296$, $p=0.004$) in the entire patient sample (Supplementary Table 2). Thus, this *p*-value did not survive Bonferroni correction for multiple testing (threshold at $p=0.0009$).

3.4. Patients vs. healthy controls

TBSS: Standard voxel-wise TBSS analyses did not reveal significant differences in FA in SSD-P or SSD-nonP patients when compared to HC ($p=0.26$ and $p=0.46$, respectively). After excluding all three covariates (age, sex, and OLZ) and performing an independent two-sample *t*-test, we found significantly lower FA in SSD-P patients when compared to HC ($p=0.03$).

Using the average FA across all 15 tracts between sensorimotor regions, Games-Howell post-hoc analysis revealed significantly lower FA in the left ST_FO ($p = 0.01$) in SSD-P patients when compared to HC. Using ANCOVA, we found no significant FA difference in CC_7 and right and left ST_FO between SSD-P or SSD-nonP patients and HC. After excluding all three covariates (age, sex, and OLZ) and performing an independent two-sample *t*-test, we found significantly lower FA in CC_6 ($p=0.041$), CC_7 ($p=0.009$), left ST_FO ($p=0.005$), and right ST_FO ($p=0.021$) in SSD-P patients when compared to HC. There were no significant differences in FA between SSD-nonP patients and HC (all *p*-values>0.066). Thus, these p-values did not survive Bonferroni correction for multiple testing (threshold at $p=0.002$).

Tractography: We found decreased FA in CC_2, CC_3, CC_4, CC_5, CC_6, CC_7 (all min. *p*-values<0.0001), the left and right T_PREM (both min. *p*-values<0.001), the left and right ST_FO (both min. *p*-values<0.002), and the right ST_PREM (min. *p*-value<0.0008) of SSD-P patients when compared to HC (all p-values below FWE-corrected threshold). We also found differences in FA in CC_1 (increased; min. *p*-value<0.001), CC_3 (decreased; min. *p*-value<0.0006), CC_7 (both decreased and increased; min. *p*-value<0.0002), left T_PREM (increased; min. *p*-value<0.000021), right ST_FO (decreased; min. *p*-value<0.000065) and left ST_PREM (decreased; min. *p*-value<0.0008) in SSD-nonP patients compared to HC (all *p*-values below alphaFWE-corrected threshold). Thus, only the minimal p-values of the SSD-P vs. HC comparison in CC_2 (threshold at $p=0.002/30=0.00006$), CC_3 (threshold at $p=0.001/30=0.00003$), CC_4 (threshold at $p=0.001/30=0.00003$), CC_5 (thresh-

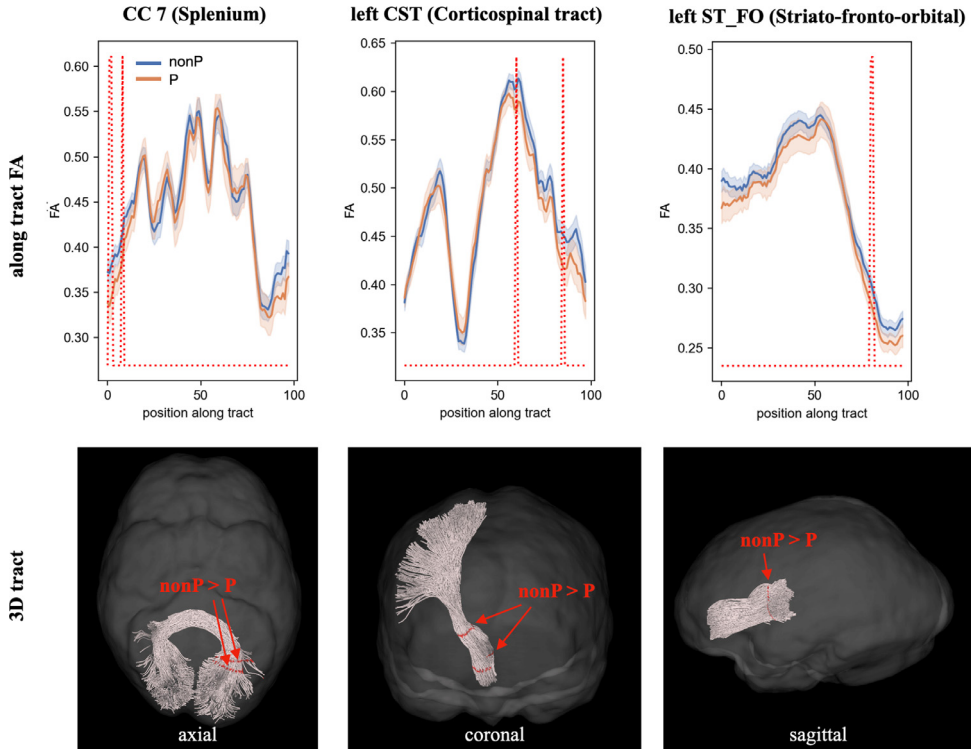

Fig. 2 Significant differences in FA between SSD patients with (P) and without (nonP) parkinsonism (Tractometry analysis; results before Bonferroni correction).

old at p=0.002/30=0.00006), CC_7 (threshold at p=0.001/30=0.00003), left T_PREM (threshold at p=0.002/30=0.00006) and left ST_FO (threshold at p=0.003/30=0.0001) survived Bonferroni correction for multiple testing. Finally, only the minimal p-value of the SSD-nonP vs. HC comparison in left T_PREM (threshold at p=0.001/30=0.00003) and right ST_FO (threshold at p=0.003/30=0.0001) survived Bonferroni correction for multiple testing.

Large-scale network analysis: ANCOVA revealed no significant differences between patient groups and HC (p>0.15) (Supplementary Table 2). After excluding all three covariates (age, sex, and OLZ) and performing an independent two-sample t-test, we found a significant increase in CCO in the right SFG in SSD-P patients compared to HC (p=0.038). There was no significant difference in CCO or BC in other brain regions between SSD-nonP patients and HC (all p-values>0.058).

4. Discussion

The present multiparametric dMRI study investigated, for the first time, brain WM microstructure abnormalities underlying parkinsonism in SSD patients. Three main findings emerged: First, we found reduced FA in left CST and ST_FO in SSD-P patients compared to SSD-nonP patients. Second, there were significant positive associations between FA in CC_5, CST and ST_FO and SAS total scores. Third, there was a significant association between CCO in left OFC and SAS total score. Although these findings did not survive conservative Bonferroni correction for multiple comparisons, we feel that it is valuable to discuss them. The specific purpose of this study was to better understand WM microstructure underlying parkinsonism. Since there are no previous studies that have used DTI to address this specific question, the consequences of a false negative, when using conservative correction thresholds for multiple comparisons, would be to miss regional WM variations of heuristic importance in relation to parkinsonism. Therefore, as false negatives are costly under these conditions, reporting and discussing uncorrected results can be valuable in such instances.

4.1. TBSS and tractography

Using an aggregated TBSS (similar to a recent study of WM microstructural differences in schizophrenia (SZ) Kelly et al., 2018), we found reduced FA in the left CST and the ST_FO in SSD-P patients compared to SSD-nonP patients. The FA decrease in CST may relate to decreased input from the thalamus and striatum or altered pallido-thalamic activity (Mole et al., 2016). Since CST carries WM motor tracts to peripheral muscular output (Du et al., 2017), distortion of structural integrity in CST might lead to aberrant inhibitory signaling and sensorimotor abnormalities. The ST_FO is a neural pathway that connects frontal lobe regions with the basal ganglia (striatum). Impaired fronto-striatal connectivity in SZ is well documented (de Leeuw et al., 2017; Levitt et al., 2017; Quan et al., 2013) and can lead to cognitive impairment (Levitt et al., 2017) as well as sensorimotor deficits such as parkinsonism (Molina et al., 2018; Wolf et al., 2020a). Interestingly, ST_FO reciprocally connects important regions involved in sensorimotor function-

ing such as the dorsolateral prefrontal cortex (DLPFC), OFC, inferior frontal gyrus, SFG and the striatum (caudate nucleus, and putamen) (de Leeuw et al., 2017). More precisely, the OFC modulates cognitive control of emotional experience and is in constant interaction with DLPFC, inferior frontal gyrus, SFG and striatum (Northoff et al., 2004). The human striatum is mainly responsible for the correct excitation of goal-directed movement schemas. Recently, an MRI study found that iron-loading measures of mainly left-side basal ganglia were associated with extrapyramidal motor symptoms and neurological soft signs (NSS) in first-episode psychosis patients (Cuesta et al., 2020). In accordance with previous findings, axon loss within the ST_FO reflects aberrant "vertical modulation" of cortico-subcortical relations, which might lead to disturbed regulation of emotional stimuli and programming and termination of action (Hirjak et al., 2015b; Northoff, 2000), as well as an imbalance between inhibitory and excitatory processes (Helmich et al., 2012; van der Stouwe et al., 2020). Taken together, these conjoint alterations in bottom-up and top-down modulation might lead to the development of typical sensorimotor abnormalities such as tremor and akinesia, which are characteristic symptoms of parkinsonism.

4.2. Large-scale network analysis

Using graph analytics, we identified significantly higher CCO values in the left OFC and left SFG in SSD-P patients compared to SSD-nonP patients. These findings are relevant for a number of reasons: First, the higher CCO of the OFC might be interpreted as a compensation mechanism for disturbed network functionality in the fronto-striatal network as represented by reduced FA in both striato-fronto-orbital tracts (SSD<HC). Such abnormalities of local efficiency can cause aberrant information transfer/processing between inhibitory and excitatory processes and hence lead to typical symptoms of parkinsonism such as rigidity and akinesia. In agreement with this, structural abnormalities in OFC have been related to the occurrence of apathy in Parkinson's disease (PD) (Martinez-Horta et al., 2017). Second, structural and functional alterations of OFC are associated with catatonia, which is a paradigmatic example of another psychomotor syndrome in SZ often characterized by hypokinesia/akinesia and flexibilitas cerea as a special type of rigidity (Hirjak et al., 2020; Walther et al., 2017; Wasserthal et al., 2020). The OFC, based on its functional connectivity with the motor cortex, can be regarded as a structure that, through top-modulation of the latter regions, leads to psychomotor abnormalities such as hypokinesia/akinesia in a truly dimensional sense, i.e. independent of underlying disorders such as major depressive disorder, bipolar disorder, or SSD (Mittal et al., 2017; Northoff et al., 2021; Northoff et al., 2004). Third, the left SFG is anatomically connected to the supplementary motor area, a region that is responsible for preparation, initiation and monitoring of action (Wolf et al., 2008). Our observations are consistent with previous studies that found SFG alterations to be involved in sensorimotor abnormalities in both HC (Hirjak et al., 2016; Thomann et al., 2015) and SSD patients (Li et al., 2013; Quispe Escudero et al., 2020). Finally, from a clinical perspective, there is some overlap between parkinsonism and catatonia in terms of rigidity, immobility or inhibited movement, psychomotor slowing, mutism, and staring. From a neurobiological perspective, the findings of the present study are in line with two recent MRI studies on catatonia in SSD (Viher et al., 2020; Wasserthal et al., 2020) that were able to demonstrate similar WM changes involving left-lateralized higher FA in the CST, CC, internal capsule and thalamo-premotor tract. These findings point towards some common pathobiology underlying catatonia and parkinsonism in SSD.

Taken together, the present FA decrease and CCO increase in different sensorimotor regions suggest a reorganization of WM fibers both as selective neurodegeneration and a resultant compensatory response in the pathogenesis of parkinsonism in SSD (Atkinson-Clement et al., 2017). Future studies should further investigate which of these mechanisms predominates and can be modulated by antipsychotic drugs.

4.3. Strengths and limitations

This study has the following strengths: (i) patient sample size, (ii) well-matched study groups, and (iii) the use of a comprehensive set of sophisticated WM microstructural parameters. However, the following methodological aspects limit the generalizability of our results: (i) Antipsychotic medication. Although antipsychotic drugs may have prominent functional effects on the identified WM tracts, our findings do not appear to be confounded by such effects because the two SSD groups were well-matched for dose in OLZ-equivalents but showed different levels of parkinsonism. This issue has also been addressed in a recent DTI study by Kraguljac and colleagues (Kraguljac et al., 2019), which found no alterations in micro- or macrostructural WM integrity after short-term treatment with risperidone. An earlier T1 study by Emsley and colleagues (Emsley et al., 2017) showed no WM abnormalities even after one year of treatment in previously antipsychotic naïve SZ patients. Interestingly, Liemburg and colleagues (Liemburg et al., 2018) found different effects of risperidone and aripiprazole on grey matter and WM volumes as well as neurometabolite levels in psychotic patients. Future large-scale studies are needed to disentangle the effects of antipsychotics with different receptor profiles on brain structure and function. Other factors, in addition to antipsychotic drug treatment, may have contributed to development of the sensorimotor dysfunction of parkinsonism, e.g. WM alterations.

Among other aspects, (ii) we did not detect any group differences in TBSS when comparing SSD patients with HC. While this may be due to the small number of HC, this finding corroborates other TBSS studies (Boos et al., 2013; Clark et al., 2012) on similar numbers of SSD patients and HC, which also did not find significant differences between them. (iii) Our DTI sequences did not include the brainstem (in favor of higher resolution of cortical structures), so we were unable to investigate brainstem nuclei that might also be involved in parkinsonism. (iv) A potential limitation of the SAS is overestimation of rigidity, because it includes a total of six items examining this specific symptom (Cuesta et al., 2014; Loonen and van Praag, 2007). However,

using the SAS as a composite score has proven to better separate specific patient groups (placebo vs. 1 mg haloperidol) than the six hypokinetic/rigidity items alone. (v) SSD patients in this study may also have had other sensorimotor abnormalities such as NSS or catatonia. However, though this study concerned both categorical and dimensional assessment of parkinsonism, there can be considerable clinical overlap with such other sensorimotor abnormalities. Therefore, we advocate that sensorimotor assessments combine both clinical ratings scales and instrumental assessments (Hirjak et al., 2021). This would help to clarify the pathophysiology of parkinsonism and other sensorimotor abnormalities from a broader perspective.

5. Conclusion

This study provides a comprehensive, state-of-the-art analysis of WM microstructure in SDD patients with and without parkinsonism that appears to reflect an interaction between sensorimotor dysfunction intrinsic to SSD and the effects of antipsychotic drugs; thus, just as movement disorder intrinsic to PD can be exacerbated by antipsychotics, parkinsonism appears to be intrinsic to SSD in a manner that can be exacerbated by these same agents (Waddington, 2020). In this regard, the main finding in the present study is that dysfunction in the topological metrics of small-world brain networks in SSD comprise sensorimotor regions such as OFC, SFG and striatum that operate in a dimensional and cross-nosological manner. This is indicated by their extents of expression being related across the triadic psychomotor abnormalities of parkinsonism, i.e. rigidity, akinesia and tremor.

6. Contributors

DH and RCW designed the study and wrote the protocol. DH, SF and LSG performed the motor assessments in all study subjects. KMK and AH managed the literature searches and analyses. JW, KMH, PH and DH undertook the statistical analysis. DH, RCW, GN, JLW and HT discussed and interpreted the results. DH wrote the first draft of the manuscript. All authors contributed to and have approved the final manuscript.

Role of funding source

This work was supported by the German Research Foundation (DFG) (grant number DFG HI 1928/2-1 to D.H., WO 1883/6-1 to R.C.W., MA 6340/10-1 and MA 6340/12-1 to K.H.M.-H.) and German Federal Ministry of Education and Research (BMBF, grant 01GQ1102 to H.T.). The DFG and BMBF had no further role in study design; in the collection, analysis and interpretation of data; in the writing of the report; and in the decision to submit the paper for publication. GN is grateful for financial support from PSI and CIHR in Canada. The authors have declared that there are no conflicts of interest in relation to the subject of this study.

Declaration of Competing Interest

The authors have declared that there are no conflicts of interest in relation to the subject of this study.

Acknowledgments

We are grateful to all the participants and their families for their time and interest in this study.

Supplementary material

Supplementary material associated with this article can be found, in the online version, at doi:10.1016/j.euroneuro.2021.04.007.

References

Andersson, J.L.R., Sotiropoulos, S.N., 2016. An integrated approach to correction for off-resonance effects and subject movement in diffusion MR imaging. NeuroImage 125, 1063–1078.

Atkinson-Clement, C., Pinto, S., Eusebio, A., Coulon, O., 2017. Diffusion tensor imaging in Parkinson's disease: review and meta-analysis. Neuroimage Clin. 16, 98–110.

Bach, M., Laun, F.B., Leemans, A., Tax, C.M.W., Biessels, G.J., Stieltjes, B., Maier-Hein, K.H., 2014. Methodological considerations on tract-based spatial statistics (TBSS). NeuroImage 100, 358–369.

Boos, H.B., Mandl, R.C., van Haren, N.E., Cahn, W., van Baal, G.C., Kahn, R.S., Hulshoff Pol, H.E., 2013. Tract-based diffusion tensor imaging in patients with schizophrenia and their non-psychotic siblings. Eur. Neuropsychopharmacol.: J. Eur. Coll. Neuropsychopharmacol. 23, 295–304.

Clark, K., Narr, K.L., O'Neill, J., Levitt, J., Siddarth, P., Phillips, O., Toga, A., Caplan, R., 2012. White matter integrity, language, and childhood onset schizophrenia. Schizophr. Res. 138, 150–156.

Cuesta, M.J., Lecumberri, P., Moreno-Izco, L., Lopez-Ilundain, J.M., Ribeiro, M., Cabada, T., Lorente-Omenaca, R., de Erausquin, G., Garcia-Marti, G., Sanjuan, J., Sanchez-Torres, A.M., Gomez, M., Peralta, V., 2020. Motor abnormalities and basal ganglia in first-episode psychosis (FEP). Psychol. Med. 1–12.

Cuesta, M.J., Sanchez-Torres, A.M., de Jalon, E.G., Campos, M.S., Ibanez, B., Moreno-Izco, L., Peralta, V., 2014. Spontaneous parkinsonism is associated with cognitive impairment in antipsychotic-naive patients with first-episode psychosis: a 6-month follow-up study. Schizophr. Bull. 40, 1164–1173.

Dale, A.M., Fischl, B., Sereno, M.I., 1999. Cortical surface-based analysis. I. Segmentation and surface reconstruction. NeuroImage 9, 179–194.

Dazzan, P., Morgan, K.D., Orr, K.G., Hutchinson, G., Chitnis, X., Suckling, J., Fearon, P., Salvo, J., McGuire, P.K., Mallett, R.M., Jones, P.B., Leff, J., Murray, R.M., 2004. The structural brain correlates of neurological soft signs in AESOP first-episode psychoses study. Brain 127, 143–153.

de Leeuw, M., Bohlken, M.M., Mandl, R.C., Hillegers, M.H., Kahn, R.S., Vink, M., 2017. Changes in white matter organization in adolescent offspring of schizophrenia patients. Neuropsychopharmacology 42, 495–501.

Desikan, R.S., Segonne, F., Fischl, B., Quinn, B.T., Dickerson, B.C., Blacker, D., Buckner, R.L., Dale, A.M., Maguire, R.P., Hyman, B.T., Albert, M.S., Killiany, R.J., 2006. An automated labeling system for subdividing the human cerebral cortex on MRI scans into gyral based regions of interest. NeuroImage 31, 968–980.

Du, X., Kochunov, P., Summerfelt, A., Chiappelli, J., Choa, F.S., Hong, L.E., 2017. The role of white matter microstructure in inhibitory deficits in patients with schizophrenia. Brain Stimul. 10, 283–290.

Emsley, R., Asmal, L., du Plessis, S., Chiliza, B., Phahladira, L., Kilian, S., 2017. Brain volume changes over the first year of treatment in schizophrenia: relationships to antipsychotic treatment. Psychol. Med. 47, 2187–2196.

Fischl, B., Dale, A.M., 2000. Measuring the thickness of the human cerebral cortex from magnetic resonance images. Proc. Natl. Acad. Sci. U. S. A. 97, 11050–11055.

Fischl, B., Sereno, M.I., Dale, A.M., 1999. Cortical surface-based analysis. II: Inflation, flattening, and a surface-based coordinate system. NeuroImage 9, 195–207.

Fischl, B., van der Kouwe, A., Destrieux, C., Halgren, E., Segonne, F., Salat, D.H., Busa, E., Seidman, L.J., Goldstein, J., Kennedy, D., Caviness, V., Makris, N., Rosen, B., Dale, A.M., 2004. Automatically parcellating the human cerebral cortex. Cereb. Cortex 14, 11–22.

Freeman, L.C., 1977. A set of measures of centrality based on betweenness. Sociometry 40, 31–40.

Fritze, Stefan, Harneit, Anais, Waddington L., John, Kubera M., Katharina, Schmitgen M., Mike, Otte, Marie-Luise, Geiger S., Lena, Tost, Heike, Meyer-Lindenberg, Andreas, Wolf C., Robert, Hirjak, Dusan, 2021. Structural alterations in brainstem, basal ganglia and thalamus associated with parkinsonism in schizophrenia spectrum disorders. European Archives of Psychiatry and Clinical Neuroscience In press.

Goch, C.J., Stieltjes, B., Henze, R., Hering, J., Poustka, L., Meinzer, H.P., Maier-Hein, K.H., 2014. Quantification of changes in language-related brain areas in autism spectrum disorders using large-scale network analysis. Int. J. Comput. Assist. Radiol. Surg. 9 (3), 357–365. doi:10.1007/s11548-014-0977-0.

Helmich, R.C., Hallett, M., Deuschl, G., Toni, I., Bloem, B.R., 2012. Cerebral causes and consequences of parkinsonian resting tremor: a tale of two circuits? Brain 135, 3206–3226.

Hirjak, D., Kubera, K.M., Northoff, G., Fritze, S., Bertolino, A.L., Topor, C.E., Schmitgen, M.M., Wolf, R.C., 2019. Cortical contributions to distinct symptom dimensions of catatonia. Schizophr. Bull. 45 (6), 1184–1194. doi:10.1093/schbul/sby192.

Hirjak, D., Kubera, K.M., Thomann, P.A., Wolf, R.C., 2018a. Motor dysfunction as an intermediate phenotype across schizophrenia and other psychotic disorders: progress and perspectives. Schizophr. Res. 200, 26–34.

Hirjak, D., Kubera, K.M., Wolf, R.C., Northoff, G., 2020. Going back to Kahlbaum's psychomotor (and GABAergic) origins: is catatonia more than just a motor and dopaminergic syndrome? Schizophr Bull. 46 (2), 272–285. doi:10.1093/schbul/sbz042.

Hirjak, D., Meyer-Lindenberg, A., Fritze, S., Sambataro, F., Kubera, K.M., Wolf, R.C., 2018b. Motor dysfunction as research domain across bipolar, obsessive-compulsive and neurodevelopmental disorders. Neurosci. Biobehav. Rev. 95, 315–335.

Hirjak, D., Meyer-Lindenberg, A., Kubera, K.M., Thomann, P.A., Wolf, R.C., 2018c. Motor dysfunction as research domain in the period preceding manifest schizophrenia: a systematic review. Neurosci. Biobehav. Rev. 87, 87–105.

Hirjak, Dusan, Meyer-Lindenberg, Andreas, Sambataro, Fabio, Wolf C., Robert, 2021. Sensorimotor Neuroscience in Mental Disorders: Progress, Perspectives and Challenges. Schizophrenia Bulletin. In press.

Hirjak, D., Rashidi, M., Kubera, K.M., Northoff, G., Fritze, S., Schmitgen, M.M., Sambataro, F., Calhoun, V.D., Wolf, R.C., 2020. Multimodal magnetic resonance imaging data fusion reveals distinct patterns of abnormal brain structure and function in catatonia. Schizophr. Bull. 46 (1). doi:10.1093/schbul/sbz042.

Hirjak, D., Thomann, P.A., Kubera, K.M., Wolf, N.D., Sambataro, F., Wolf, R.C., 2015a. Motor dysfunction within the schizophrenia-spectrum: a dimensional step towards an underappreciated domain. Schizophr. Res. 169, 217–233.

Hirjak, D., Thomann, P.A., Kubera, K.M., Wolf, N.D., Sambataro, F., Wolf, R.C., 2015b. Motor dysfunction within the schizophrenia-spectrum: a dimensional step towards an underappreciated domain. Schizophr. Res. 169, 217–233.

Hirjak, D., Wolf, R.C., Kubera, K.M., Stieltjes, B., Thomann, P.A., 2016. Multiparametric mapping of neurological soft signs in healthy adults. Brain Struct. Funct. 221, 1209–1221.

Jenkinson, M., Beckmann, C.F., Behrens, T.E., Woolrich, M.W., Smith, S.M., 2012. FSL. NeuroImage 62, 782–790.

Jenkinson, M., Smith, S., 2001. A global optimisation method for robust affine registration of brain images. Med. Image Anal. 5, 143–156.

Kellner, E., Dhital, B., Kiselev, V.G., Reisert, M., 2016. Gibbs-ringing artifact removal based on local subvoxel-shifts. Magn. Reson. Med.: Off. J. Soc. Magn. Reson. Med./Soc. Magn. Reson. Med. 76, 1574–1581.

Kelly, S., Jahanshad, N., Zalesky, A., Kochunov, P., Agartz, I., Alloza, C., Andreassen, O.A., Arango, C., Banaj, N., Bouix, S., Bousman, C.A., Brouwer, R.M., Bruggemann, J., Bustillo, J., Cahn, W., Calhoun, V., Cannon, D., Carr, V., Catts, S., Chen, J., Chen, J.X., Chen, X., Chiapponi, C., Cho, K.K., Ciullo, V., Corvin, A.S., Crespo-Facorro, B., Cropley, V., De Rossi, P., Diaz-Caneja, C.M., Dickie, E.W., Ehrlich, S., Fan, F.M., Faskowitz, J., Fatouros-Bergman, H., Flyckt, L., Ford, J.M., Fouche, J.P., Fukunaga, M., Gill, M., Glahn, D.C., Gollub, R., Goudzwaard, E.D., Guo, H., Gur, R.E., Gur, R.C., Gurholt, T.P., Hashimoto, R., Hatton, S.N., Henskens, F.A., Hibar, D.P., Hickie, I.B., Hong, L.E., Horacek, J., Howells, F.M., Hulshoff, P., Hyde, H.E., Isaev, C.L., Jablensky, D., Jansen, A., Janssen, P.R., Jonsson, J., Jung, E.G., Kahn, L.A., Kikinis, R.S., Liu, Z., Klauser, K., Knochel, P., Kubicki, C., Lagopoulos, M., Langen, J., Lawrie, C., Lenroot, S., Lim, R.K., Lopez-Jaramillo, K.O., Lyall, C., Magnotta, A., Mandl, V., Mathalon, R.C.W., McCarley, D.H., McCarthy-Jones, R.W., McDonald, S., McEwen, C., McIntosh, S., Melicher, A., Mesholam-Gately, T., Michie, R.I., Mowry, P.T., Mueller, B., Newell, B.A., O'Donnell, D.T., Oertel-Knochel, P., Oestreich, V., Paciga, L., Pantelis, S.A., Pasternak, C., Pearlson, O., Pellicano, G., Pereira, G.R., Pineda Zapata, A., Piras, J., Potkin, F., Preda, S.G., Rasser, A., Roalf, P.E., Roiz, D.R., Roos, R., Rotenberg, A., Satterthwaite, D., Savadjiev, T.D., Schall, P., Scott, U., Seal, R.J., Seidman, M.L., Shannon, L.J., Weickert, ., Whelan, C., Shenton, C.D., Kwon, M.E., Spalletta, J.S., Spaniel, G., Sprooten, F., Stablein, E., Stein, M., Sundram, D.J., Tan, S., Tan, Y., Tang, S., Temmingh, S., Westlye, H.S., Tonnesen, L.T., Tordesillas-Gutierrez, S., Doan, D., Vaidya, N.T., van Haren, J., Vargas, N.E.M, Vecchio, C.D., Velakoulis, D., Voineskos, D., Voyvodic, A., Wang, J.Q., Wan, Z., Wei, P., Weickert, D., Whalley, T.W., White, H., Whitford, T., Wojcik, T.J., Xiang, J.D., Xie, H., Yamamori, Z., Yang, H., Yao, F., Zhang, N., Zhao, G., van Erp, J., Turner, T.G.M., Thompson, J., Donohoe, P.M., 2018. Widespread white matter microstructural differences in schizophrenia across 4322 individuals: results from the ENIGMA Schizophrenia DTI Working Group. Mol. Psychiatry 23, 1261–1269.

Kraguljac, N.V., Anthony, T., Skidmore, F.M., Marstrander, J., Morgan, C.J., Reid, M.A., White, D.M., Jindal, R.D., Melas Skefos, N.H., Lahti, A.C., 2019. Micro- and macrostructural white matter integrity in never-treated and currently unmedicated patients with schizophrenia and effects of short-term antipsychotic treatment. Biol. Psychiatry Cognit. Neurosci. Neuroimaging 4, 462–471.

Leucht, S., Samara, M., Heres, S., Patel, M.X., Furukawa, T., Cipriani, A., Geddes, J., Davis, J.M., 2015. Dose equivalents for second-generation antipsychotic drugs: the classical mean dose method. Schizophr. Bull. 41, 1397–1402.

Levitt, J.J., Nestor, P.G., Levin, L., Pelavin, P., Lin, P., Kubicki, M., McCarley, R.W., Shenton, M.E., Rathi, Y., 2017. Reduced structural connectivity in frontostriatal white matter tracts in the associative loop in schizophrenia. Am. J. Psychiatry 174, 1102–1111.

Li, C.T., Chou, K.H., Su, T.P., Huang, C.C., Chen, M.H., Bai, Y.M., Lin, C.P., 2013. Gray matter abnormalities in schizophrenia patients with tardive dyskinesia: a magnetic resonance imaging voxel-based morphometry study. PLoS One 8, e71034.

Liemburg, E.J., Sibeijn-Kuiper, A., Knegtering, H., Aleman, A., 2018. The effect of aripiprazole versus risperidone on prefrontal brain metabolite levels and brain volume in psychotic disorders: an exploratory study. Neuropsychiatry 8, 176–185.

Loonen, A.J., van Praag, H.M., 2007. Measuring movement disorders in antipsychotic drug trials: the need to define a new standard. J. Clin. Psychopharmacol. 27, 423–430.

Martinez-Horta, S., Sampedro, F., Pagonabarraga, J., Fernandez-Bobadilla, R., Marin-Lahoz, J., Riba, J., Kulisevsky, J., 2017. Non-demented Parkinson's disease patients with apathy show decreased grey matter volume in key executive and reward-related nodes. Brain Imaging Behav. 11, 1334–1342.

Mittal, V.A., Bernard, J.A., Northoff, G., 2017. What can different motor circuits tell us about psychosis? An RDoC perspective. Schizophr. Bull. 43, 949–955.

Mole, J.P., Subramanian, L., Bracht, T., Morris, H., Metzler-Baddeley, C., Linden, D.E., 2016. Increased fractional anisotropy in the motor tracts of Parkinson's disease suggests compensatory neuroplasticity or selective neurodegeneration. Eur. Radiol. 26, 3327–3335.

Molina, V., Lubeiro, A., Blanco, J., Blanco, J.A., Rodriguez, M., Rodriguez-Campos, A., de Luis-Garcia, R., 2018. Parkinsonism is associated to fronto-caudate disconnectivity and cognition in schizophrenia. Psychiatry Res. Neuroimaging 277, 1–6.

Neher, P.F., Descoteaux, M., Houde, J.C., Stieltjes, B., Maier-Hein, K.H., 2015. Strengths and weaknesses of state of the art fiber tractography pipelines – a comprehensive in-vivo and phantom evaluation study using tractometer. Med. Image Anal. 26, 287–305.

Nichols, T.E., Holmes, A.P., 2002. Nonparametric permutation tests for functional neuroimaging: a primer with examples. Hum. Brain Mapp. 15, 1–25.

Northoff, G., 2000. Brain imaging in catatonia: current findings and a pathophysiologic model. CNS Spectr. 5, 34–46.

Northoff, G., 2002. What catatonia can tell us about "top-down modulation": a neuropsychiatric hypothesis. Behav. Brain Sci. 25, 555–577 discussion 578–604.

Northoff, G., Hirjak, D., Wolf, R.C., Magioncalda, P., Martino, M., 2021. All roads lead to the motor cortex: psychomotor mechanisms and their biochemical modulation in psychiatric disorders. Mol. Psychiatry 26 (1), 92–102. doi:10.1038/s41380-020-0814-5.

Northoff, G., Kotter, R., Baumgart, F., Danos, P., Boeker, H., Kaulisch, T., Schlagenhauf, F., Walter, H., Heinzel, A., Witzel, T., Bogerts, B., 2004. Orbitofrontal cortical dysfunction in akinetic catatonia: a functional magnetic resonance imaging study during negative emotional stimulation. Schizophr. Bull. 30, 405–427.

Oldfield, R.C., 1971. The assessment and analysis of handedness: the Edinburgh inventory. Neuropsychologia 9, 97–113.

Pappa, S., Dazzan, P., 2009. Spontaneous movement disorders in antipsychotic-naive patients with first-episode psychoses: a systematic review. Psychol. Med. 39, 1065–1076.

Peralta, V., Basterra, V., Campos, M.S., de Jalon, E.G., Moreno-Izco, L., Cuesta, M.J., 2012. Characterization of spontaneous Parkinsonism in drug-naive patients with nonaffective psychotic disorders. Eur. Arch. Psychiatry Clin. Neurosci. 262, 131–138.

Quan, M., Lee, S.H., Kubicki, M., Kikinis, Z., Rathi, Y., Seidman, L.J., Mesholam-Gately, R.I., Goldstein, J.M., McCarley, R.W., Shenton, M.E., Levitt, J.J., 2013. White matter tract abnormalities between rostral middle frontal gyrus, inferior frontal gyrus and striatum in first-episode schizophrenia. Schizophr. Res. 145, 1–10.

Quispe Escudero, D., Herold, C.J., Kong, L., Schroder, J., 2020. Neurological soft signs (NSS) and gray matter volume (GMV) in first-episode psychosis: an analysis of NSS motor subscores. Psychiatry Res. Neuroimaging 300, 111067.

Rubinov, M., Bullmore, E., 2013. Fledgling pathoconnectomics of psychiatric disorders. Trends Cognit. Sci. 17, 641–647.

Sass, H., Wittchen, H.U., Zaudig, M., I., H., 2003. Diagnostisches und Statistisches Manual Psychischer Störungen DSM-IV-TR: Textrevision, 1. Hogrefe Verlag Auflage(1. Januar 2003).

Segonne, F., Dale, A.M., Busa, E., Glessner, M., Salat, D., Hahn, H.K., Fischl, B., 2004. A hybrid approach to the skull stripping problem in MRI. NeuroImage 22, 1060–1075.

Simpson, G.M., Angus, J.W., 1970. A rating scale for extrapyramidal side effects. Acta Psychiatr. Scand. Suppl. 212, 11–19.

Smeland, O.B., Shadrin, A., Bahrami, S., Broce, I., Tesli, M., Frei, O., Wirgenes, K.V., O'Connell, K.S., Krull, F., Bettella, F., Steen, N.E., Sugrue, L., Wang, Y., Svenningsson, P., Sharma, M., Pihlstrom, L., Toft, M., O'Donovan, M., Djurovic, S., Desikan, R., Dale, A.M., Andreassen, O.A., 2021. Genome-wide association analysis of Parkinson's disease and schizophrenia reveals shared genetic architecture and identifies novel risk loci. Biol. Psychiatry 89 (3), 227–235. doi:10.1016/j.biopsych.2020.01.026.

Smith, R.E., Tournier, J.D., Calamante, F., Connelly, A., 2015. The effects of SIFT on the reproducibility and biological accuracy of the structural connectome. NeuroImage 104, 253–265.

Smith, S.M., 2002. Fast robust automated brain extraction. Hum. Brain Mapp. 17, 143–155.

Smith, S.M., Jenkinson, M., Johansen-Berg, H., Rueckert, D., Nichols, T.E., Mackay, C.E., Watkins, K.E., Ciccarelli, O., Cader, M.Z., Matthews, P.M., Behrens, T.E., 2006. Tract-based spatial statistics: voxelwise analysis of multi-subject diffusion data. NeuroImage 31, 1487–1505.

Thomann, P.A., Hirjak, D., Kubera, K.M., Stieltjes, B., Wolf, R.C., 2015. Neural network activity and neurological soft signs in healthy adults. Behav. Brain Res. 278, 514–519.

Tustison, N.J., Avants, B.B., Cook, P.A., Zheng, Y., Egan, A., Yushkevich, P.A., Gee, J.C., 2010. N4ITK: improved N3 bias correction. IEEE Trans. Med. Imaging 29, 1310–1320.

van der Stouwe, M., Nieuwhof, F., Helmich, R.C., 2020. Tremor pathophysiology: lessons from neuroimaging. Curr. Opin. Neurol. 33 (4), 474–481. doi:10.1097/WCO.0000000000000829.

Veraart, J., Novikov, D.S., Christiaens, D., Ades-Aron, B., Sijbers, J., Fieremans, E., 2016. Denoising of diffusion MRI using random matrix theory. NeuroImage 142, 394–406.

Viher, P.V., Stegmayer, K., Federspiel, A., Bohlhalter, S., Wiest, R., Walther, S., 2020. Altered diffusion in motor white matter tracts in psychosis patients with catatonia. Schizophr. Res. 220, 210–217.

Waddington, J.L., 2020. Psychosis in Parkinson's disease and parkinsonism in antipsychotic-naive schizophrenia spectrum psychosis: clinical, nosological and pathobiological challenges. Acta Pharmacol. Sin. 41, 464–470.

Walther, S., Schappi, L., Federspiel, A., Bohlhalter, S., Wiest, R., Strik, W., Stegmayer, K., 2017. Resting-state hyperperfusion of the supplementary motor area in catatonia. Schizophr. Bull. 43, 972–981.

Walther, S., van Harten, P.N., Waddington, J.L., Cuesta, M.J., Peralta, V., Dupin, L., Foucher, J.R., Sambataro, F., Morrens, M., Kubera, K.M., Pieters, L.E., Stegmayer, K., Strik, W., Wolf, R.C., Hirjak, D., 2020. Movement disorder and sensorimotor abnormalities in schizophrenia and other psychoses – European consensus on assessment and perspectives. Eur. Neuropsychopharmacol.: J. Eur. Coll. Neuropsychopharmacol.

Wassermann, D., Rathi, Y., Bouix, S., Kubicki, M., Kikinis, R., Shenton, M., Westin, C.F., 2011. White matter bundle registration and population analysis based on Gaussian processes. Inf. Process. .Med Imaging 22, 320–332.

Wasserthal, J., Maier-Hein, K.H., Neher, P.F., Northoff, G., Kubera, K.M., Fritze, S., Harneit, A., Geiger, L.S., Tost, H., Wolf, R.C., Hirjak, D., 2020. Multiparametric mapping of white matter microstructure in catatonia. Neuropsychopharmacology 45 (10), 1750–1757. doi:10.1038/s41386-020-0691-2.

Wasserthal, J., Neher, P., Maier-Hein, K.H., 2018. TractSeg - Fast and accurate white matter tract segmentation. NeuroImage 183, 239–253.

Wasserthal, J., Neher, P.F., Hirjak, D., Maier-Hein, K.H., 2019. Combined tract segmentation and orientation mapping for bundle-specific tractography. Med. Image Anal. 58, 101559.

Whitty, P.F., Owoeye, O., Waddington, J.L., 2009. Neurological signs and involuntary movements in schizophrenia: intrinsic to and informative on systems pathobiology. Schizophr. Bull. 35, 415–424.

Wolf, R.C., Hose, A., Frasch, K., Walter, H., Vasic, N., 2008. Volumetric abnormalities associated with cognitive deficits in patients with schizophrenia. Eur. Psychiatry 23, 541–548.

Wolf C., Robert, Kubera M., Katharina, Waddington L., John, Schmitgen M., Mike, Fritze, Stefan, Rashidi, Mahmoud, Thieme E., Cristina, Sambataro, Fabio, Geiger S., Lena, Tost, Heike, Hirjak, Dusan, 2021. A neurodevelopmental signature of parkinsonism in schizophrenia.. Schizophr Res. 54–60. doi:10.1016/j.schres.2021.03.004.

Wolf, R.C., Rashidi, M., Fritze, S., Kubera, K.M., Northoff, G., Sambataro, F., Calhoun, V.D., Geiger, L.S., Tost, H., Hirjak, D., 2020a. A neural signature of parkinsonism in patients with schizophrenia spectrum disorders: a multimodal MRI study using parallel ICA. Schizophr. Bull. 46, 999–1008.

Wolf, R.C., Rashidi, M., Fritze, S., Kubera, K.M., Northoff, G., Sambataro, F., Calhoun, V.D., Geiger, L.S., Tost, H., Hirjak, D., 2020b. A neural signature of parkinsonism in patients with schizophrenia spectrum disorders: a multimodal MRI study using parallel ICA. Schizophr. Bull 46 (4), 999–1008. doi:10.1093/schbul/sbaa007.

Woolrich, M.W., Jbabdi, S., Patenaude, B., Chappell, M., Makni, S., Behrens, T., Beckmann, C., Jenkinson, M., Smith, S.M., 2009. Bayesian analysis of neuroimaging data in FSL. NeuroImage 45, S173–S186.

Yeatman, J.D., Dougherty, R.F., Myall, N.J., Wandell, B.A., Feldman, H.M., 2012. Tract profiles of white matter properties: automating fiber-tract quantification. PLoS One 7, e49790.

Yeatman, J.D., Dougherty, R.F., Rykhlevskaia, E., Sherbondy, A.J., Deutsch, G.K., Wandell, B.A., Ben-Shachar, M., 2011. Anatomical properties of the arcuate fasciculus predict phonological and reading skills in children. J. Cognit. Neurosci. 23, 3304–3317.